An Experimental Investigation of Stone Mastic Asphalt Reinforced with Nanoclay-Modified Sisal Fiber

Godfred Kankam
Department of Civil Engineering, Pan African University Institute for Basic Sciences, Technology and Innovation, Kenya
godfred.kankam@students.jkuat.ac.ke (corresponding author)

Kiplagat Chelelgo
Department of Civil Engineering, Dedan Kimathi University of Technology, Kenya
kiplagat.chelelgo@dkut.ac.ke

M'Tulatia Mungathia
Department of Civil, Construction and Environmental Engineering, Jomo Kenyatta University of Agriculture and Technology, Kenya
mungathiatulatia@jkuat.ac.ke

Received: 21 February 2026 | Revised: 15 March 2026 | Accepted: 26 March 2026

 DOI: https://doi.org/10.48084/etasr.18308

ABSTRACT

Stone Mastic Asphalt (SMA) is a gap-graded, bituminous mixture with a stone-on-stone skeleton and a high binder content. This composition provides superior load-bearing capacity and rutting resistance. However, the gap-graded nature and high binder content of SMA make it susceptible to binder drain-down. Although natural fibers are considered a sustainable additive for reinforcement, their organic and hydrophilic properties raise concerns about high moisture absorption, which could reduce the long-term durability of SMA. This study examined nanoclay-modified, sisal fiber-reinforced SMA, focusing on volumetric design, moisture resistance, and binder draindown. The materials used include aggregates, sisal fiber, Organically Modified Montmorillonite (OMMT) nanoclay, and Styrene-Butadiene-Styrene (SBS)-modified bitumen. The Superpave procedure was adopted to design an SMA with a nominal maximum aggregate size of 12.5 mm. The optimum binder content that yielded the desired air voids was 6.6%. The sisal fiber content varied from 0% to 0.5% of the total weight of the SMA mixtures. Then, OMMT nanoclay was applied as a modifier to the sisal fiber before it was incorporated into the SMA. Sisal modification was performed at OMMT levels of 0%, 2%, 4%, 6%, and 8%. The optimum sisal fiber content was 0.3%, yielding a Tensile Strength Ratio (TSR) of 85.6% and a draindown of 0.08%. OMMT-modified, sisal-reinforced SMA produced an improved TSR of 96.5% and reduced draindown to 0.05%. These results demonstrate that modifying sisal with nanoclay improves the binder retention and moisture resistance of asphalt mixtures.

Keywords-stone mastic asphalt; organically modified montmorillonite; sisal fiber

I. INTRODUCTION

Stone Mastic Asphalt (SMA) is a specialized bituminous mixture with a gap-graded structure that is typically produced at high temperatures [1]. Its stone-on-stone skeleton structure and rich mastic give SMA a high load-bearing capacity and rutting resistance. These properties have made SMA popular for use on roads with high traffic capacity, including major highways and airport runways [2, 3]. Unlike dense-graded mixtures, SMA contains a higher proportion of coarse aggregates (typically 70-80%), bitumen (6-7%), and filler (8-12%) [4, 5]. The evolution of SMA dates back to the mid-1960s in Germany and has since gained global recognition [6]. A long-term pavement performance assessment in the United States showed that SMA has a longer service life and yields a 69.3% return on investment compared to dense-graded asphalt mixtures over 29 years [7]. However, the stone-on-stone structure that gives SMA its strength creates binder draindown and stability issues, especially at high temperatures and steep gradients during placement and transportation [8]. To mitigate these issues, stabilizing additives, such as mineral, cellulose, and synthetic fibers, have been explored [9]. Adopting

sustainable materials has led to the exploration of natural fibers as environmentally friendly alternatives [10, 11]. Sisal fiber, obtained from the Agave sisalana plant, is a good option, with wide availability, eco-friendly, and favorable mechanical properties [12-14]. However, sisal's hydrophilic and organic nature introduces challenges related to moisture uptake, affecting the mixture's durability, particularly under wet conditions [15, 16]. Nanomaterials are promising options for improving the performance of composite materials [17, 18]. Organically Modified Montmorillonite (OMMT) nanoclay can enhance cohesion, reduce moisture permeability, and improve adhesion in composite systems [19, 20]. Its layered silicate structure creates tortuous paths that hinder moisture ingress, improving its water barrier properties [15]. Authors in [21, 22] incorporated nanoclay directly into the asphalt binder; this approach primarily targets the bulk binder phase. Authors in [17] highlighted the modification of the asphalt binder's elastic behavior. In contrast, the present study introduces OMMT nanoclay as a surface modifier for sisal fiber before SMA addition. This places the nanoclay at the critical fiber-mastic interface, rather than dispersing it throughout the bulk binder, creating a localized moisture barrier on the hydrophilic fiber surface. Thus, more efficient use of the nanomaterial is offered while addressing the specific moisture susceptibility of natural fiber reinforcement in SMA. Consequently, the current study evaluates the effect of OMMT modification on moisture susceptibility and draindown in SMA.

II. MATERIALS AND METHODS

A. Materials

The materials used in this study are: stone aggregates, Styrene-Butadiene-Styrene (SBS) modified bitumen, sisal fiber, and OMMT nanoclay. The coarse and fine aggregates, sized 0/3 mm, 0/6 mm, 6/10 mm, and 10/14 mm, were from the H-Young Katani Quarry in Machakos County, Kenya. The mineral filler was obtained by sieving the 0/3 mm aggregate fraction through a 0.075 mm sieve in the laboratory. Batra Kenya Limited supplied SBS-modified 50/70 penetration grade bitumen containing 4.5% SBS polymer, which was used as the binder for the SMA mixtures. OMMT nanoclay was procured from Ultrananotech Private Limited in India. Sisal fibers were sourced locally from Don's Fiber in Ngong, Kenya. The fibers were pretreated with a 5% sodium hydroxide solution to remove surface impurities and improve compatibility with the asphalt matrix.

B. Method

The study followed the AASHTO R46 [23] and Asphalt Institute MS-2 [24] guidelines to design the SMA mixtures. The Superpave design procedure was adopted, as proposed by NAPA [25].

1) Aggregate Gradation

The aggregate gradation was tested according to the Asphalt Institute's MS-2 [24] guidelines in order to achieve a 12.5 NMAS SMA. Since SMA has a gap-graded structure, it requires a higher proportion of coarse aggregates (retained on a 4.75-mm sieve), a higher proportion of fine aggregates (passing a 0.075-mm sieve), and a bitumen content of 6-7%. These proportions ensure stone-on-stone contact and a rich mastic, providing satisfactory consistency in the mix [25]. The single-size aggregates used were 10/14 mm, 6/10 mm, and 0/6 mm, as well as fillers (0/0.075 mm). After grading the single-size aggregates, a simple analytical method was adopted, targeting the midpoint of the specified gradation limits for each sieve to determine the proportions of each aggregate size required. Various sizes were blended, in order to produce a gradation that meets the required SMA specifications [24]:

$$P = aA + bB + cC \quad (1)$$

where P is the combined percentage passing a given sieve, A, B, and C are the percentages passing a sieve for an individual stockpile, and a, b, and c are the proportions of the individual stockpile added to the blend. To achieve the desired stone-on-stone contact for SMA, the voids in the coarse aggregate fraction of the aggregate blend (VCA_{drc}) must exceed the voids in the coarse aggregate within the compacted mix (VCA_{mix}). The VCA is evaluated according to AASHTO T19 [26] using:

$$VCA_{drc} = \left(\frac{G_{CA}\gamma_w - \gamma_s}{G_{CA}\gamma_s}\right) \times 100 \quad (2)$$

where G_{CA} is the bulk specific gravity of the coarse aggregate, γ_w is the unit weight of water, and γ_s is the dry-rodded unit weight of the coarse aggregate fraction.

2) Design Binder Content

SMA samples were prepared using a Superpave gyratory compactor. A mold with a diameter of 150 mm was utilized. The initial binder content (P_{bi}) was estimated according to SHRP-A-4-7 [27] using:

$$P_{bi} = \frac{G_b(V_{be} + V_{ba})}{G_b(V_{be} + V_{ba}) + W_s} \quad (3)$$

where G_b is the specific gravity of bitumen, V_{be} is the volume fraction of effective bitumen content, V_{ba} is the estimated fraction volume of bitumen that will be absorbed by aggregates, and W_s is the fraction of total mixture volume contributed by aggregate solids. The analysis revealed an initial bitumen content estimate of 5.9%. Five trial bitumen contents were evaluated: 4.9%, 5.4%, 5.9%, 6.4%, and 6.9%. The theoretical maximum specific gravities of each trial mix were determined using AASHTO T209 [28]. Three replicates of each trial bitumen content were compacted using a design number of gyrations (N_{design}) of 100, as proposed by NAPA for SMA. This implies an initial number of gyrations ($N_{initial}$) and a maximum number of gyrations (N_{max}) of eight and 160, respectively. The N_{design} target is for medium-to-high traffic volumes ranging from 3 - 30 MSA over a 20-year design period. The bulk specific gravity of the compacted SMA mixtures was determined using the saturated surface-dry specimen method in accordance with AASHTO T166 [29]. The volumetric properties of the SMA samples were determined using the Gmm and Gmb values acquired. The evaluated properties included the percentage of air voids (V_a), Voids in Mineral Aggregates (VMA), and VCA_{mix}. V_a, VCA_{mix}, and VMA were calculated using:

$$V_a = 100 - \left(100 \times \frac{G_{mb}}{G_{mm}}\right) \quad (4)$$

$$VCA_{mix} = 100 - (P_{CA} \times \frac{G_{mb}}{G_{CA}}) \quad (5)$$

$$VMA = 100 - (P_s \times \frac{G_{mb}}{G_{sb}}) \quad (6)$$

where G_{mb} is the bulk specific gravity of compacted mixture, $G_{mm\,is}$ the theoretical maximum specific gravity of the mixture, P_{CA} is the percent of coarse aggregates in the mixture, G_{CA} is the bulk specific gravity of coarse aggregate fraction, Ps is the percentage of aggregate in the mix, and G_{sb} is the bulk specific gravity of combined aggregate. The design bitumen content was determined according to the criteria outlined in AASHTO M325 [30]. The bitumen content corresponding to 4% air voids was chosen as the design binder content. This content was maintained for all modified mixtures to isolate the effects of fiber reinforcement and OMMT modification, ensuring that the volumetric properties remained within acceptable limits.

3) Modification of Sisal Fiber with OMMT Nanoclay

In order to modify the sisal fiber with OMMT nanoclay, the fiber was cut into 6 mm lengths to ensure uniform dispersion and functionality [31, 32]. The fibers were rinsed with distilled water to reduce the alkaline concentration. OMMT nanoclay was then dissolved in distilled water at varying percentages (0%, 2%, 4%, 6%, and 8%, by weight, of the fiber). The fiber was added to the nanoclay solution and stirred continuously with a high-shear mixer for 3 h to promote uniform surface coating. The fibers were then removed and dried at 60 °C for 24 h. Scanning Electron Microscopy (SEM) images were used to verify the modification of the sisal fiber with OMMT nanoclay.

4) Resistance to Moisture Induced Damage

In accordance with AASHTO T283 [33], the resistance to moisture damage of sisal-reinforced SMA was determined. Then, the effect of OMMT modification on the moisture resistance of the SMA mixture was evaluated. The modified Lottman procedure was adopted to determine the mixture's Tensile Strength Ratio (TSR). To achieve 7% air voids, % G_{mm} was plotted against the log of the number of gyrations, as proposed by AIMS-2 [24]. The number of gyrations (N), corresponding to 93% G_{mm}, was used to compact the mixtures for Indirect Tensile Strength (ITS). Based on Figure 1 and laboratory confirmation, 40 gyrations were used to achieve 7±0.5% air voids, and the mixture was then compacted to a height of 95 ± 5 mm. Six replicates were prepared for each set, and the compacted samples were divided into two subsets of three each. The first subset was conditioned, while the second remained unconditioned. The specimens in the conditioned subset were subjected to vacuum saturation until reaching 55–80% saturation. Then, they were immersed in a 60°C water bath for 24 h, in accordance with AASHTO T283 [33]. Then, both the conditioned and unconditioned specimens were brought to 25°C prior to ITS testing, which was conducted at a loading rate of 50 mm/min for both the conditioned and unconditioned samples. The maximum load (P) was recorded from the test, and the ITS was:

$$ITS = \frac{2P}{\pi DT} \quad (7)$$

where P (kN) is the maximum load recorded at failure, D (mm) is the diameter of the specimen, and T (mm) is the thickness of the specimen. *TSR* represents the ability of the SMA mixture to resist moisture-induced damage and retain strength during moisture conditioning. It is calculated as the ratio of ITS of conditioned samples to ITS of unconditioned samples, and the minimum proposed value by AIMS-2 is 80%:

$$TSR = \frac{ITS_{conditioned}}{ITS_{unconditioned}} \quad (8)$$

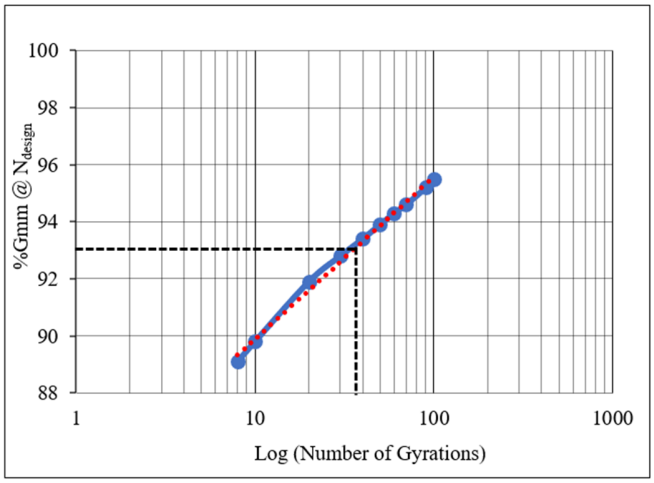

Fig. 1. Theoretical max specific gravity against number of gyrations.

5) Binder Draindown

Binder draindown is an important parameter in gap-graded and open-graded asphalt mixtures, such as SMA, affecting binder retention and stability [34, 35]. According to AASHTO M325 [30], the binder draindown in an SMA mixture should not exceed 0.3%. To determine the extent of bitumen drainage in SMA mixtures, a drainage test was conducted in accordance with AASHTO T305 [36]. Uncompacted SMA mixtures weighing 1,200 grams were prepared at the optimum binder content. The sample was placed in a 6.3 mm sieve-sized metal basket with a tray of known weight beneath it. The setup was placed in an oven at 175 °C for 1 h. Draindown values are determined by:

$$Draindown = 100 \times \left(\frac{A - B}{C}\right) \quad (9)$$

where A is the final weight of tray (g) after 1 hour, B is the initial weight of tray (g), and C is the initial sample weight (g).

III. RESULTS AND DISCUSSION

A. Material Characterisation

1) Aggregate

The elemental composition and properties of the aggregates are presented in Tables I and II, respectively. X-ray Fluorescence (XRF) spectroscopy analysis reveals a silica-rich aggregate containing 65.7% SiO_2 and significant amounts of Al_2O_3 and K_2O, suggesting a granitic origin of the aggregates. The aggregate properties satisfy the proposed requirements for aggregates used in asphalt mixtures.

TABLE I. CHEMICAL COMPOSITION OF AGGREGATE

Chemical composition	Percentage in aggregates (%)
SiO_2	65.734
Al_2O_3	18.083
K_2O	8.576
Fe	5.134
CaO	1.705
Ti	0.747
Mn	0.364
Cl	0.297
P_2O_5	0.093
Others	0.267

TABLE II. PHYSICAL PROPERTIES OF AGGREGATE

Property	Test procedure	Value
Bulk specific gravity (kg/m^3)	ASTM C127	2.596
Los Angeles abrasion (%)	ASTM C131	23
Aggregate impact value (%)	BS 812	18
Moisture absorption (%)	ASTM C127	2.3

2) Bitumen

The properties of the SBS-modified bitumen, including penetration, specific gravity, and softening point, are presented in Table III. These properties demonstrate that the binder possesses adequate stiffness and thermal stability, making it suitable for use in SMA mixtures.

TABLE III. PROPERTIES OF SBS-MODIFIED BITUMEN

Property	Test procedure	Value
Penetration (dmm)	ASTM D5	59
Specific gravity (g/cm^3)	ASTM D70	1.03
Softening point (°C)	ASTM D36	51
Elastic recovery (%)	ASTM D6084	81

3) Organically Modified Montmorillonite Nanoclay

The properties and chemical composition of the OMMT, as determined by XRF spectrometry, are presented in Tables IV and V. The high purity, moderate specific gravity, and d-spacing of 3.4 nm indicate that OMMT nanoclay is well-suited for effective dispersion and interaction with fibers. OMMT nanoclay's chemical composition shows that it is mostly silica-rich with significant alumina content, which is characteristic of montmorillonite clay.

TABLE IV. PROPERTIES OF ORGANICALLY MODIFIED NANOCLAY

Property	Value
Purity (%)	99.5
Specific gravity (g/cm^3)	1.7
XRD d001 (nm)	3.4

TABLE V. CHEMICAL COMPOSITION OF ORGANICALLY MODIFIED NANOCLAY

Chemical composition	Percentage in OMMT
SiO_2	75.37
Al_2O_3	11.57
CaO	5.36
MgO	4.23
K_2O	2.45
Others	1.03

4) Sisal Fiber

As shown in Table VI, the small diameter and moderate density of sisal fiber suggest that it can effectively disperse in SMA, allowing sisal to act as a reinforcing additive in the mixture.

TABLE VI. PROPERTIES OF SISAL FIBER

Property	Test procedure	Value
Diameter (mm)		0.13
Water absorption (%)	ASTM D570	95
Density (g/cm^3)	ASTM D792	1.37

B. Stone Mastic Asphalt Aggregate Gradation

The aggregate proportions were 10% for 10/14 mm, 63% for 6/10 mm, 20% for 0/6 mm, and 7% for the filler. Following the AIMS-2 guidelines [24], the adopted gradation of the SMA mixture, as displayed in Figure 2, is within the specified limits, confirming the gap-graded structure, necessary for stone-on-stone contact in the SMA mixture.

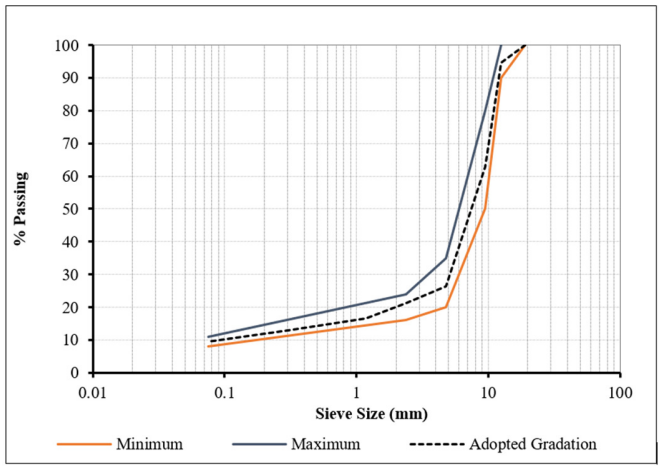

Fig. 2. SMA aggregate gradation.

C. Design Binder Content

The design binder content was determined to be the amount of binder that corresponded to 4% air voids. As the binder content increased, the air void content decreased from 8% at 4.9% to 3.2% at 6.9%. This decrease is attributed to the progressive filling of the air spaces between the aggregate particles as binder content increases. This results in denser packing of the SMA mix. As shown in Figure 3, the desired air void content of 4% was achieved at an OBC of 6.6%. These findings are consistent with those reporting that the typical binder content for SMA mixtures ranges between 6.0% and 7.0%. Table VII outlines the SMA mixture properties at the design binder content of 6.6%. The volumetric properties satisfy the requirements of AASHTO M325. The mixture achieved 4.0% air voids, with VCA_{mix} less than VCA_{drc}, which confirms stone-on-stone contact. The *VMA* exceeded the minimum of 17%, validating the selected gradation and design binder content for the SMA mixture.

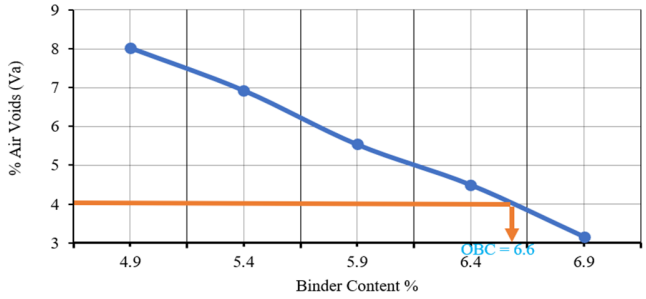

Fig. 3. Determination of design binder content.

TABLE VII. VOLUMETRIC PROPERTIES OF SMA AT OBC

Property	Value	Requirement per AASHTO M325
G_{mm}	2.408	
G_{mb}	2.311	
Percent air voids (% V_a)	4.0	4.0
VCA_{drc} (%)	44.9	
VCA_{mix} (%)	38.95	< VCA_{drc}
VMA (%)	17.6	min

D. Organically Modified Montmorillonite Modification of Sisal Fiber

SEM and Energy Dispersive Spectroscopy (EDS) confirmed the presence of OMMT particles on OMMT-modified sisal fibers. EDS confirmed the absence of silica in unmodified sisal fibers and its presence in various OMMT-modified sisal fibers. Figures 4 and 5 illustrate SEM images of sisal and OMMT-modified sisal, respectively, zoomed 300 times at 50 µm resolution. OMMT-modified sisal fiber shows barrier structures created by OMMT nanoclay particles.

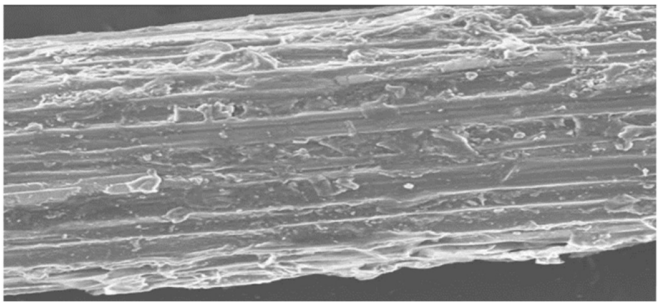

Fig. 4. SEM image of unmodified sisal fiber at 300 times zoom, 5 kV, and 50 µm resolution.

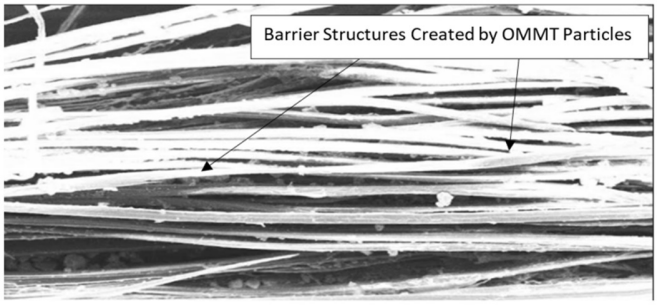

Fig. 5. SEM image of OMMT modified sisal fiber at 300 times zoom, 5 kV, and 50 µm resolution.

The sisal fiber had a relatively smooth surface, while the OMMT-modified sisal fibers had a rougher surface with barrier structures. This indicates successful nanoclay deposition on the fiber. Nanoclay coatings create tortuous paths where the platelet morphology of OMMT particles forms barrier structures that impede moisture ingress. The increased surface roughness enhances fiber-mastic interfacial interaction through improved mechanical interlocking. However, advanced characterization, such as Fourier Transform Infrared (FTIR), was not conducted to quantitatively verify the bonding mechanisms or the coating thickness. Therefore, the proposed barrier effects are inferred from morphological observations and performance in an asphalt mixture.

E. Effect of Nanoclay Modification of Sisal Fiber on Moisture Resistance of Stone Mastic Asphalt

The ITS test was used to evaluate the resistance of the SMA mixture to moisture-induced damage by measuring its TSR. As shown in Figure 6, at 0% fiber content, the SMA mixture exhibited a TSR of 71.3%, indicating lower moisture resistance at this level. The 28.7% reduction in the tensile strength of the conditioned SMA mixture suggests a loss of internal cohesion and a weakening of the mastic due to moisture ingress. The mixture exhibited continuous improvement in TSR as fiber content increased. The optimum sisal fiber content is 0.3%, at which the SMA mixture achieved a TSR value of 85.6%. This improvement is attributed to the reinforcing ability of sisal fibers, which play a key role in stress distribution and enhance structural integrity and crack bridging. The improvement in TSR demonstrates the mixture's ability to resist moisture-induced damage. However, the SMA mixture exhibited a decline in TSR beyond 0.3%. This decline suggests the onset of fiber clustering and reduced compaction efficiency within the SMA mixture [37]. As reported in fiber-reinforced mixtures, excessive fiber dosage can lead to uneven dispersion and agglomeration during mixing, weakening internal cohesion within the asphalt mixture. The observed reduction in TSR is consistent with the findings in [13, 38], indicating that excessive fiber content weakens the internal structure of the mixture, resulting in reduced performance.

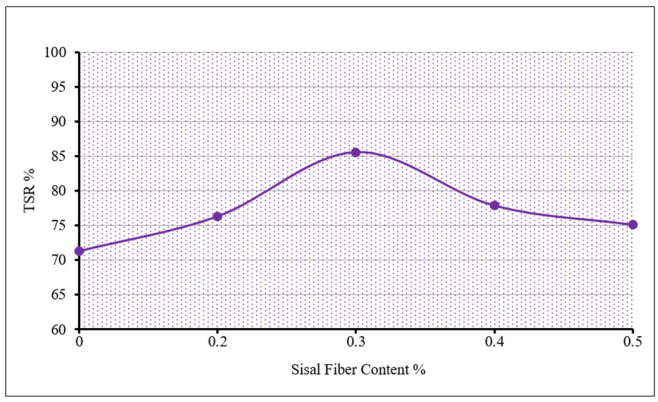

Fig. 6. Tensile strength ratios at varying sisal content.

Figure 7 depicts the moisture resistance of the OMMT-sisal SMA composite. Modifying sisal with OMMT progressively

improved its moisture resistance. The optimal level of OMMT modification was 4%, at which the SMA mixture achieved a TSR value of 96.5%. This indicates improved resistance to moisture-induced damage compared to sisal SMA, showing a 10.7% improvement in TSR over sisal SMA. The high TSR of the OMMT-sisal SMA mixture indicates high strength retention under moisture conditioning. This improvement suggests reduced binder permeability and limited moisture ingress due to the barrier structures created by nanoclay particles. However, a decline in TSR beyond a 4% OMMT level suggests the possibility of nanoclay agglomeration and uneven dispersion on the sisal, which could lead to stress concentration in the SMA mixture. The 4% OMMT-modified sisal fiber shows enhanced strength retention and moisture durability in the SMA mixture. This demonstrates the ability of OMMT nanoclay to create a moisture barrier on sisal. Authors in [15, 39] observed the strong moisture barrier properties of nanoclays. However, the interaction of nanoclay within the bulk binder phase was not directly evaluated. Therefore, the observed enhancement is mainly attributed to the surface modification of the sisal fiber rather than to the alteration of the bulk binder.

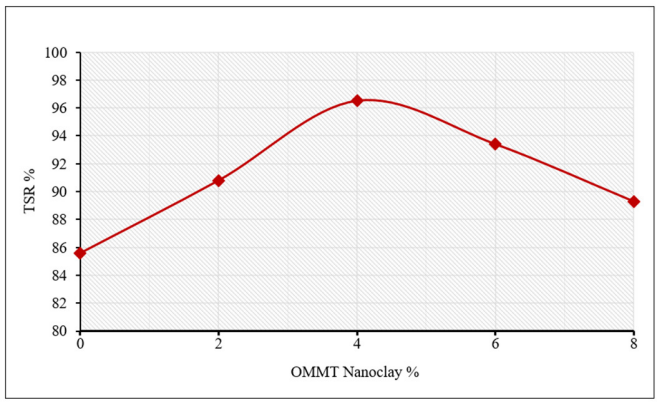

Fig. 7. Tensile strength ratios at varying OMMT modification levels.

To validate this observation, a one-way ANOVA was conducted on the TSR results, revealing a statistically significant difference among mixtures with different levels of OMMT modification ($F = 91.80$, $p < 0.0001$). This indicates that OMMT content significantly affects the moisture resistance of SMA mixtures. Tukey's HSD post hoc test also confirmed that the 4% OMMT-modified sisal SMA, with a TSR of 96.5%, was significantly higher than all other modification levels ($p < 0.01$). The 2% and 8% levels, however, were statistically equivalent. These results statistically validate 4% OMMT as the optimal modification level.

F. Effect of Nanoclay Modification of Sisal Fiber on Binder Draindown of Stone Mastic Asphalt

The draindown of the SMA indicates its binder retention ability. The optimal dosage of sisal fiber yielded a draindown of 0.08%. This is due to binder absorption by the sisal fiber and the physical entrapment of the binder within the fiber network. As shown in Figure 8, OMMT modification of the sisal fiber further reduced the draindown in the SMA mixture, resulting in nearly zero draindown. This additional reduction is attributed to the micro-barrier effect created by the nanoclay coating, revealing the significant role of sisal fiber in controlling draindown. Authors in [35, 40] reported fiber as the primary mechanism for draindown control in SMA mixtures, while OMMT nanoclay contributes to additional binder stabilization. Statistical analysis using one-way ANOVA confirmed that the level of OMMT modification significantly affected binder draindown ($p < 0.0001$), demonstrating that the reduction in draindown observed at varying levels of OMMT modification is statistically significant.

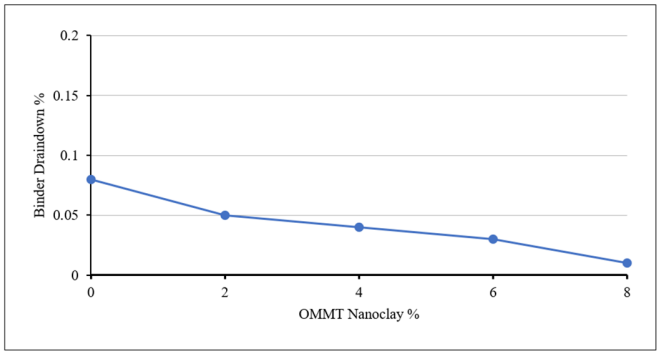

Fig. 8. Draindown of SMA at varying OMMT modification levels.

IV. CONCLUSIONS

This study investigated Organically Modified Montmorillonite (OMMT)-modified, sisal fiber-reinforced Stone Mastic Asphalt (SMA). The study focused on moisture resistance and binder drainage, as these are critical concerns for natural fiber-reinforced SMA. Due to its gap-graded structure, SMA inherently requires fibers to stabilize the binder [34], while the hydrophilic nature of sisal fiber necessitates establishing the mixture's moisture resistance [4]. Based on the study's findings:

- The optimum binder content that satisfies the volumetric requirements for air voids, Voids in Mineral Aggregates (VMA), and voids in coarse aggregates, in accordance with SMA design criteria, is 6.6%. This confirms that the selected aggregate gradation and binder content successfully established the required stone-on-stone skeleton structure and adequate mastic volume.
- The optimum sisal fiber content was achieved at 0.3% of the total mix weight, yielding a Tensile Strength Ratio (TSR) of 85.6% and a draindown of 0.08%. This improvement is attributed to the fiber's ability to bridge micro-cracks and physically entrap the binder within its network. This improves draindown and mitigates moisture damage.
- Modifying the sisal fiber with OMMT further improved moisture resistance. This modification yielded a TSR of 96.5% and reduced draindown to 0.05%. One-way ANOVA analysis confirmed that nanoclay modification of sisal fiber significantly improved the SMA mixture's

resistance to moisture-induced damage and binder draindown.

- Although the nanoclay modification of the fiber may increase the complexity and cost of processing, the performance of the mixture may offset the initial expenses. A detailed cost-benefit analysis is proposed for future work. Additionally, future studies should evaluate the mixture's mechanical performance, including fatigue and aging behavior, alongside advanced microstructural analysis to validate its practical viability.

DECLARATION OF COMPETING INTERESTS

The authors declare that they have no competing financial or personal interests that could have influenced the research paper.

ACKNOWLEDGMENT

The authors sincerely acknowledge the African Union Commission for financially supporting the research through the Pan African University Institute for Basic Sciences, Technology, and Innovation (PAUSTI). The authors also acknowledge the Materials Testing and Research Directorate of Kenya's Ministry of Transport for providing laboratory facilities and technical support. Appreciation is also extended to the Pan African University Institute for Basic Sciences, Technology, and Innovation, and Jomo Kenyatta University of Agriculture and Technology for their institutional support and conducive academic environment.

DATA AVAILABILITY

The data used in this study consist mainly of laboratory experimental data and are available from the corresponding author upon reasonable request.

REFERENCES

[1] Q. Huang, Z. Qian, J. Hu, and D. Zheng, "Evaluation of stone mastic asphalt containing ceramic waste aggregate for cooling asphalt pavement," *Materials*, vol. 13, no. 13, 2020, Art. no. 2964, https://doi.org/10.3390/ma13132964.

[2] S. A. Tayh and H. S. J. Alghrery, "Evaluation of the effect of gradation on mechanical properties of stone mastic asphalt mixtures," *IOP Conference Series: Materials Science and Engineering*, vol. 1105, no. 1, 2021, Art. no. 012087, https://doi.org/10.1088/1757-899X/1105/1/012087.

[3] F. Morea, R. Nosetti, L. Gonzalez, and A. Sánchez, "Performance analysis of non-conventional stone mastic asphalt elaborated with crumb rubber bitumen or by means of glass macrofibers addition," *Construction and Building Materials*, vol. 400, 2023, Art. no. 132654, https://doi.org/10.1016/j.conbuildmat.2023.132654.

[4] S. Singh *et al.*, "Preference Index of Sustainable Natural Fibers in Stone Matrix Asphalt Mixture Using Waste Marble," *Materials*, vol. 15, no. 8, Jan. 2022, Art. no. 2729, https://doi.org/10.3390/ma15082729.

[5] K. A. Tutu, C. A. Nketiah, M. Owusu, and M. F. Baidoo, "Advancing stone matrix asphalt sustainability through full replacement of conventional aggregates with steel slag and palm kernel shell ash," *International Journal of Pavement Research and Technology*, 2025, https://doi.org/10.1007/s42947-025-00505-8.

[6] H. Wu, P. Xiao, Z. Fei, A. Kang, and X. Wu, "Evaluation of SMA-13 asphalt mixture reinforced by different types of fiber additives," *Materials*, vol. 17, no. 22, 2024, Art. no. 5468, https://doi.org/10.3390/ma17225468.

[7] J. Lee, J. Jeon, A. Mamun, M. Khajehvand, and J. Haddock, "Stone Matrix Asphalt (SMA) Overlay Performance Evaluation," Joint Transportation Research Program, West Lafayette, IN, USA, Technical FHWA/IN/JTRP-2025/09, Jan. 2025. https://doi.org/10.5703/1288284317853.

[8] S. Eskandarsefat, B. Hofko, and C. Sangiorgi, "A comparison study on low-temperature properties of stone mastic asphalts modified with PmBs or modified fibres," *International Journal of Pavement Engineering*, vol. 21, no. 12, pp. 1541–1549, 2020, https://doi.org/10.1080/10298436.2018.1554219.

[9] M. Irfan, Y. Ali, S. Ahmed, S. Iqbal, and H. Wang, "Rutting and fatigue properties of cellulose fiber-added stone mastic asphalt concrete mixtures," *Advances in Materials Science and Engineering*, vol. 2019, 2019, Art. no. 5604197, https://doi.org/10.1155/2019/5604197.

[10] I. AlSaadi, S. A. Tayh, A. F. Jasim, and R. Yousif, "The use of natural fibers in stone mastic asphalt mixtures: A review of the literature," *Archives of Civil Engineering*, vol. 69, no. 3, 2023. https://doi.org/10.24425/ace.2023.146085.

[11] T. D. K. A. Masri and A. O. A. Baqadeem, "Fibers in asphalt mixture: A state-of-the-art review," *Construction*, vol. 3, no. 1, pp. 115–122, 2023, https://doi.org/10.15282/construction.v3i1.9215.

[12] P. Parimita, "Influence of natural fibers as additive on characteristics of stone mastic asphalt," *IOP Conference Series: Materials Science and Engineering*, vol. 970, no. 1, 2020, Art. no. 012021, https://doi.org/10.1088/1757-899X/970/1/012021.

[13] M. Razahi and A. Chopra, "An experimental investigation of using sisal fiber and coir fiber as an additive in stone matrix asphalt," *International Journal of Advance Science and Technology*, vol. 29, no. 10S, pp. 5111–5128, 2020.

[14] H. M. A. A. Kareem and A. H. K. Albayati, "The Possibility of Minimizing Rutting Distress in Asphalt Concrete Wearing Course," *Engineering, Technology & Applied Science Research*, vol. 12, no. 1, pp. 8063–8074, Feb. 2022, https://doi.org/10.48084/etasr.4669.

[15] T. P. Mohan and K. Kanny, "Water barrier properties of nanoclay filled sisal fibre reinforced epoxy composites," *Composites Part A: Applied Science and Manufacturing*, vol. 42, no. 4, pp. 385–393, 2011, https://doi.org/10.1016/j.compositesa.2010.12.010.

[16] T. A. da Silveira *et al.*, "Synergistic Effects of Furfurylated Natural Fibers and Nanoclays on the Properties of Fiber–Cement Composites," *Ceramics*, vol. 8, no. 2, June 2025, Art. no. 68, https://doi.org/10.3390/ceramics8020068.

[17] A. Amini, "Effect of nanoclay on the rheological properties, rutting, fatigue, and storage stability of polymer-modified binder," *Journal of Materials in Civil Engineering*, vol. 37, no. 6, 2025, https://doi.org/10.1061/JMCEE7.MTENG-19376.

[18] A. Amini, H. Ziari, S. A. Saadatjoo, N. S. Hashemifar, and A. Goli, "Rutting resistance, fatigue properties and temperature susceptibility of nano clay modified asphalt rubber binder," *Construction and Building Materials*, vol. 267, 2021, Art. no. 120946, https://doi.org/10.1016/j.conbuildmat.2020.120946.

[19] S. C. Mallampati *et al.*, "A study on the effect of nanoclay addition on the erosion wear characteristics of S-glass/sisal reinforced hybrid polymer composites," *Discover Materials*, vol. 4, no. 1, Nov. 2024, Art. no. 82, https://doi.org/10.1007/s43939-024-00149-8.

[20] I. D. Ibrahim, T. Jamiru, E. R. Sadiku, W. K. Kupolati, and S. C. Agwuncha, "Impact of surface modification and nanoparticle on sisal fiber reinforced polypropylene nanocomposites," *Journal of Nanotechnology*, vol. 2016, 2016, Art. no. 4235975, https://doi.org/10.1155/2016/4235975.

[21] F. C. G. Martinho and J. P. S. Farinha, "An overview of the use of nanoclay-modified bitumen in asphalt mixtures for enhanced flexible pavement performances," *Road Materials and Pavement Design*, vol. 20, no. 3, pp. 671–701, 2019, https://doi.org/10.1080/14680629.2017.1408482.

[22] B. Yilmaz, A. M. Özdemir, and H. E. Gürbüz, "Assessment of thermal properties of nanoclay-modified bitumen," *Arabian Journal for Science and Engineering*, vol. 48, no. 4, pp. 4595–4607, 2023, https://doi.org/10.1007/s13369-022-07142-4.

[23] *R 46-08 - Designing Stone Matrix Asphalt (SMA)*. Washington DC, USA: AASHTO, 2012.

[24] *Asphalt Mix Design Methods MS-2*, 7th ed. Lexington, KY, USA: Asphalt Institute, 2014.

[25] *Designing and Constructing SMA Mixtures: State-of-the-Practice*. Lanham, MD, USA: National Asphalt Pavement Association (NAPA), 2002.

[26] *C29/C29M-17a Standard Test Method for Bulk Density in Aggregates*. Washington DC, USA: AASHTO, 2018.

[27] *Superpave Mix Design Manual: SHRP A 407 for New Construction*. Washington DC, USA: SHRP, 1994.

[28] *T 209-19 Standard method of test for theoretical maximum specific gravity (Gmm) and density of asphalt mixtures*. Washington DC, USA: AASHTO, 2023.

[29] *T166-13: Bulk Specific Gravity Test for HMA*. Washington, D.C., USA: AASHTO, 2022.

[30] *M 325-08 Standard Specification for Stone Matrix Asphalt (SMA)*. Washington DC, USA: AASHTO, 2012.

[31] N. Kumar R. and V. Sunitha, "Experimental investigation of stone mastic asphalt with sisal fiber," *International Journal of Engineering Research and Technology*, vol. 5, no. 11, pp. 546–550, 2016, https://doi.org/10.17577/IJERTV5IS110309.

[32] N. Benzannache, A. Bezazi, H. Bouchelaghem, M. Boumaaza, F. Scarpa, and S. Amziane, "Effects of adding sisal and glass fibers on the mechanical behaviour of concrete polymer," *Journal of Building Materials and Structures*, vol. 5, no. 1, pp. 86–94, 2018, https://doi.org/10.34118/jbms.v5i1.47.

[33] *T 283-22 Standard method of test for resistance of compacted asphalt mixtures to moisture-induced damage*. Washington DC, USA: AASHTO, 2022.

[34] L. Devulapalli, G. Sarang, and S. Kothandaraman, "Characteristics of aggregate gradation, drain down and stabilizing agents in stone matrix asphalt mixtures: A state of the art review," *Journal of Traffic and Transportation Engineering (English Edition)*, vol. 9, no. 2, pp. 167–179, 2022, https://doi.org/10.1016/j.jtte.2021.10.007.

[35] A. Sharma, R. Choudhary, and A. Kumar, "Laboratory investigation of draindown behavior of open-graded friction-course mixtures containing banana and sugarcane bagasse natural fibers," *Transportation Research Record*, vol. 2678, no. 1, pp. 366–380, 2024, https://doi.org/10.1177/03611981231170875.

[36] *T 305 Draindown characteristics in uncompacted asphalt mixtures*. Washington DC, USA: AASHTO, 2022.

[37] S. Yang, Z. Zhou, and K. Li, "Influence of fiber type and dosage on tensile property of asphalt mixture using direct tensile test," *Materials*, vol. 16, no. 2, 2023, Art. no. 822, https://doi.org/10.3390/ma16020822.

[38] B. H. Dinh, D.-W. Park, and T. M. Phan, "Healing performance of granite and steel slag asphalt mixtures modified with steel wool fibers," *KSCE Journal of Civil Engineering*, vol. 22, no. 6, pp. 2064–2072, 2018, https://doi.org/10.1007/s12205-018-1660-8.

[39] N. Saboo, M. Sukhija, and G. Singh, "Effect of nanoclay on physical and rheological properties of waste cooking oil-modified asphalt binder," *Journal of Materials in Civil Engineering*, vol. 33, no. 3, 2021, https://doi.org/10.1061/(ASCE)MT.1943-5533.0003598.

[40] A. Sharma, R. Choudhary, A. Kumar, and S. B. Dash, "Optimizing agro-based natural fiber parameters to address binder drainage in open-graded asphalt friction course mixes employing response surface methodology," *Journal of Testing and Evaluation*, vol. 53, no. 3, pp. 674–698, 2025, https://doi.org/10.1520/JTE20240301.